Cellulose (2012) 19:843–853
DOI 10.1007/s10570-012-9662-z

Cellulosic nanoparticles from alfa fibers (*Stipa tenacissima*): extraction procedures and reinforcement potential in polymer nanocomposites

Ayman Ben Mabrouk · Hamid Kaddami · Sami Boufi · Fouad Erchiqui · Alain Dufresne

Received: 23 November 2011 / Accepted: 2 February 2012 / Published online: 14 February 2012

Abstract The microstructure and chemical composition of alfa (*Stipa tenacissima*) were investigated. The polysaccharide and lignin contents were around 70 and 20 wt%, respectively. From the bleached and delignified fibers, two types of nanosized cellulosic particles were extracted, namely cellulose nanocrystals and microfibrillated cellulose (MFC). The former correspond typically to the elementary crystallite units of the cellulose fibers, with a rod-like morphology and an aspect ratio of about 20. The latter, mechanically disintegrated from oxidized bleached fibres, presents an entangled fibrillar structure with widths in the range 5-20 nm. The reinforcing potential of the ensuing nanoparticles was investigated by casting a mixture of acrylic latex and aqueous dispersion of cellulose nanoparticles. Thermo-mechanical analysis revealed a huge enhancement of the stiffness above the glass transition of the matrix. Significant differences in the mechanical reinforcing capability of the nanoparticles were reported.

Keywords Alfa · Structure · Nanocrystals · Microfibrillated cellulose (MFC) · Nanocomposites

A. B. Mabrouk · S. Boufi
Laboratoire Sciences des Matériaux et Environnement, LMSE, University of Sfax, BP 802-3018 Sfax, Tunisia

H. Kaddami
Laboratoire de Chimie Organométallique et Macromoléculaire - Matériaux Composites, Cadi Ayyad University, Faculty of Sciences and Technologies of Marrakesh, Avenue Abdekrim Elkhattabi, BP549, Marrakesh, Morocco

F. Erchiqui
Laboratoire de Plasturgie et Nanocomposites, Université de Québec en Abitibi-Témiscaminque, Boulevard de l'Université, Rouyn-Noranda, QC J9X5E4, Canada

A. Dufresne (✉)
The International School of Paper, Print Media and Biomaterials (Pagora), Grenoble Institut of Technology, BP65, 38402 Saint Martin d'Hères Cedex, France
e-mail: Alain.Dufresne@pagora.grenoble-inp.fr

Introduction

Alfa, also named Esparto grass, is an endemic gray grass plant constituting the main biomass source in semi-arid ecosystems of the south western Mediterranean basin, namely in North Africa and south of Spain. It covers a large area estimated to about 7 million ha (Algeria: 4,000,000 ha, Morocco: 3,186,000 ha, Tunisia 400,000 ha, Libya 350,000 ha, Spain: 300,000 ha.) (Terre et Vie 2002). Thanks to roots being deeply buried in the soil, it presents a high capacity of acclimatization to limited water resource, good resistance to extreme droughts and thermal stress, as well as relatively indifference to the substratum on which it grows. Alfa plants play a key role in protecting and maintaining the ecological integrity of the whole ecosystem by preventing the soil from being exposed

to wind erosion during dry periods. In addition to its physiological properties, alfa is characterized by its soft touch, interesting physical and mechanical properties that favor its exploitation to conceive items ranging from rope and baskets to beehives, traditional dwellings, market huts, mats, screens, baskets; fans and carpets. Presently, Alfa is mainly used, particularly in Tunisia, as a source of non-woody pulp intended for paper-making industry, specifically the one intended for cigarette, luxury paper, and industrial filters. However, given its high cellulose content, around 50%, application as filler in thermoplastic matrix based composites can be considered.

It is well known that cellulose is a linear polysaccharide macromolecule aggregated in the form of thin microfibrils with typical cross sections around 3.5–10 nm consisting of elementary crystallites that still aggregate in the microfibrils which may be viewed as a string of cellulose crystals linked along the microfibril axis by disordered amorphous domains. Partial release of these microfibrils can be obtained by submitting aqueous dispersions of lignocellulosic fibers to high shear forces in a conventional homogenizer in which the suspension is passed through a thin slit. The ensuing material is usually called microfibrillated cellulose (MFC). Cellulose nanocrystals (CNC) or whiskers can be prepared by dissolving the amorphous or less ordered regions of the microfibrils by acid degradation. The resulting isolated crystalline regions are typically 200–400 nm in length but some specific sources such as tunicin display nanocrystals as long as 1 μm (Dufresne 2008). Compared to CNC, MFC has a much higher aspect ratio and occurs as a web-like structure.

Polymeric nanocomposites successfully integrate the two concepts of composites and nanometer sized materials. It is accepted that the term "nanocomposite" describes a class of two-phase materials where one of the phases has at least one dimension lower than 100 nm. Typical reinforcing agents include silica beads, clay and other dispersible colloidal particles (Motomatsu et al. 1997; Pit et al. 1996; Frisch and Mark 1996; Ruckenstein and Yuan 1997; Kaddami et al. 2004; Kaddami et al. 2006). Most commercial interest in fillers for nanocomposites has focused on clay, silica and other inorganic based materials, although carbon nanotubes have also found some applications (Okada et al. 1990; Harris 2004; Lau et al. 2006). Recent reviews reported the properties and application in the nanocomposite field of CNC (Azizi Samir et al. 2005) and MFC (Sirò and Plackett 2010).

In this paper, another approach toward the valorization of alfa fibers, consisting of the extraction of two types of nanosized cellulosic particles, viz. CNC and MCF, is presented. This study is part of a larger project aiming at developing natural plants of North Africa like palm tree and alfa by extracting cellulose-based components with added value. The extraction procedures and the morphological characteristics of the ensuing nanoparticles are presented. The present study was to bring a contribution on the comparison between the reinforcing effects of CNC and MFC.

Experimental part

Materials

Chemical composition of the fibers

Alfa fibers (*Alfa tenassissima*) were harvested from the middle east of Tunisia. The chemical composition of the dried alfa fibers was determined according to the French Standards (NF T 12-011). It allows determining the weight fraction of cellulose, hemicelluloses, lignin, extractives and ashes.

Preparation of cellulose nanocrystals (CNC)

Alfa fibers were ground to a fine powder and extracted for 24 h in the soxhlet reflux of a solvent mixture composed of toluene/ethanol (62/38 v/v). This material was submitted to an alkaline treatment with a 5 wt% NaOH solution for 2 h at 80 °C under mechanical stirring. This treatment was repeated twice. The fibers were subsequently filtered and rinsed with distilled water. A subsequent bleaching treatment was performed twice at 70 °C for 1 h. The bleaching solution (pH 4.8) contained equal parts of aqueous chlorite (1.7 wt% $NaClO_2$ in water) and an acetate buffer (27 g NaOH and 75 ml glacial acetic acid, diluted to 1L using distilled water). The fibers were again filtered and rinsed with distilled water between each treatment step. The fibers were subsequently dried for 24 h at 40 °C in a convection oven and dispersed in 65 wt% sulfuric acid. This suspension was held at 60 °C under mechanical stirring for 45 min to allow hydrolysis of amorphous cellulosic domains.

The dispersion was subsequently diluted with an equal part of cold water and washed by successive centrifugations at 10,000 rpm and 10 °C until a turbid supernatant became visible (3 times). Dialysis against distilled water was performed to remove free acid in the dispersion. This was verified by neutrality of the dialysis effluent. Complete dispersion of the CNC was obtained by a sonication step using a Branson sonifier. The dispersions were stored in the refrigerator after addition of several drops of chloroform. Determination of the CNC content was done by weighing aliquots of the solution before and after drying.

Preparation of microfibrillated cellulose (MFC)

In order to facilitate the fibrillation process, the bleached alfa fibers were submitted to TEMPO-mediated oxidation under neutral condition according to the method reported by Saito et al. (2009). Cellulose fibers (5 g) were dispersed in a 0.05 M sodium phosphate buffer (500 mL, pH 7) solution, containing TEMPO (25 mg) and NaBr (250 mg). Sodium chlorite (80%, 1.13 g, 10 mmol) solution and a 2 M sodium hypochlorite solution (0.5 mL, 1.0 mmol) were added in a first step to the flask. The flask was then stirred at 500 rpm and 60 °C for a time period of 3 h. During the oxidation process, the coloration of the mixture turned into yellow owing to the generation of free chlorine. The oxidation was stopped by adding 100 mL of ethanol, and oxidized fibers were filtered and washed two times. After cooling the suspension to room temperature, the oxidized cellulose was thoroughly washed with water and then filtrated.

MFC was prepared from this material by pumping through a GEA Homogenizer processor (NS1001L PANDA 2 K-GEA, Italy). The homogenization was conducted in two steps. First, the fiber suspension at a concentration of 1.5 wt% was passed several times at a pressure of 300 bar through thin slits of the equipment, until the viscosity of the slurry increased. Then the fibrillation was pursued by 6 passes at a pressure of 600 bar.

Fraction of the unfibrillated materials

Centrifugation of a dilute MFC suspension was shown to be an efficient mean to separate the unfibrillated materials (Besbes et al. 2011) according to the following. A dilute suspension with about 0.1 wt% solid content (Sc) was centrifuged at 4,000 rpm for 20 min to separate the nanofibrillated material (in supernatant fraction) from the non-fibrillated or partially fibrillated one, which settles down. Then, the sediment fraction was dried to a constant weight at 90 °C in a halogen desiccator. The yield was calculated from Eq. 1:

$$\text{Yield } \% = \left(1 - \frac{\text{weight of dried sediment}}{(\text{weight of diluted sample} \times \ \% \text{ Sc})}\right) \times 100. \quad (1)$$

The results represent the average values of the three replications.

Acrylic polymer matrix

A commercial latex obtained by the copolymerization of styrene (S) (50 wt%) and butyl acrylate (BA) (50 wt%), was kindly provided by MPC-Prokim (Tunisia). The aqueous suspension contained spherical particles with an average diameter around 140 nm and had a 50 wt% solid fraction. The glass–rubber transition temperature (Tg) of the poly(S-co-BA) copolymer was around 25 °C. The latex was used as received.

Processing of nanocomposites

Nanocomposite films were prepared from acrylic reinforced by various percentages of CNC or MFC extracted from Alfa. The two aqueous dispersions were first mixed to obtain dry films around 1 mm thick after water evaporation. The amount of the nanofiller in the dry film was varied from 0 to 15 wt%. The mixture was mixed using a magnetic stirrer for 8 h. Prior evaporation of water was done using a rotavapor before casting the mixture in Teflon Petri vessel. The films were dried in a ventilated oven at 40 °C for 2 or 3 days depending on the amount of filler in the film. Further drying of the films was performed under vacuum at 40 °C for 12 h. The samples were codified as AP-NCX and AP-MFX for CNC and MFC-based nanocomposites, respectively, where X corresponds to the filler content by weight.

Experimental methods

Scanning electron microscopy (SEM)

SEM was used to investigate the morphology of the different types of materials and the filler/matrix interface by using ABT-55 microscope (ISI, USA). The specimens were frozen under liquid nitrogen, fractured, mounted, coated with gold/palladium and observed using an applied accelerating voltage of 10 kV.

X-ray diffraction

Alfa fibers were chopped into fine particles and compressed into disks using a cylindrical steel mold (15 mm in diameter) with an applied pressure of 32 MPa. A Philips X'Pert diffractometer fitted with a ceramic X-ray diffraction tube was used to determine the crystallinity of the fibers. The diffracted intensity of CuKα radiation (wavelength 0.1542 nm) was recorded between $2\theta = 5°$ and 40° at 40 kV and 40 mA. Several methods are proposed in the literature to determine the crystallinity index (CrI) from X-ray diffraction experiments. One of the most known and simplest physical methods was published by (Segal et al. 1959) that we used in this study to calculate the CrI of the lignocellulosic fibers. By this empirical method, the CrI is given by the following relation:

$$\mathrm{Cr}I = \frac{I_{002} - I_{\mathrm{am}}}{I_{002}} \times 100 \quad (1)$$

where I_{002} is the maximum intensity (in arbitrary units) of the 002 lattice diffraction and I_{am} is the intensity of diffraction in the same units at $2\theta = 18°$.

Transmission electron microscopy (TEM)

TEM images of alfa nanocrystals were taken with a Philips CM200 transmission electron microscope with an acceleration voltage of 80 kV. Nanocrystals were deposited from an aqueous dispersion on a microgrid (200 mesh, Electron Microscopy Sciences, Hatfield, PA, USA) covered with a thin carbon film ($\sim$200 nm). The deposited whiskers were subsequently stained with a 2% uranyl acetate solution to enhance the contrast.

Field-emission scanning electron microscopy (FE-SEM)

A Weiss SEM was used to capture secondary electron images of the surface of MFC. A drop of the MFC suspension (with a solid content about 0.2 wt%) was deposited on a surface of silicon wafer and coated with a thin Au–Pd layer applied by sputtering with a thickness being limited to 2–3 nm. To ensure good image resolution without any damage of the samples during the analysis, the acceleration voltage was maintained at a relatively low range (0.5–1 kV).

Dynamic mechanical analysis (DMA)

DMA measurements were carried out with an RSA3 apparatus from TA Instruments working in tensile mode. The specimens were thin rectangular strips with dimensions around 40 mm × 5 mm × 1 mm. Tests were performed under isochronal conditions at 1 Hz and the temperature was varied between −60 °C and 100 °C by steps of 2 °C.

Results and discussion

Morphological investigation of the fibers

Scanning electron micrographs of longitudinal and transversal cross-section of alfa fibers are presented in Fig. 1a, b, respectively. These micrographs clearly show two components, i.e. sclerenchyma fibers (died cells or mature cells or tracheids) and conducting vessels. The detailed structure of slot as well as of the fiber bundles is shown in Fig. 1c–f. The vessels are wrapped in a bundle of fibers (or surrounded with fibers). The width of the vessel could reach 20 µm. The diameter of the fibers varies from 5 to 10 µm. These results are consistent with those reported by Röser and Heklau (2011) and Bessadok et al. (2007).

The slot through the bulk fiber that better reveals the inner surface of the plant has a very peculiar structure (Fig. 1g, h) that is detailed in Fig. 1i, j. Indeed, analysis of the inner surface of the fiber slit shown in detail the emergence of a multitude of tips homogeneously distributed with regular spectacular forms. The chemical analysis of these tips, using EDX-SEM, revealed their inorganic composition

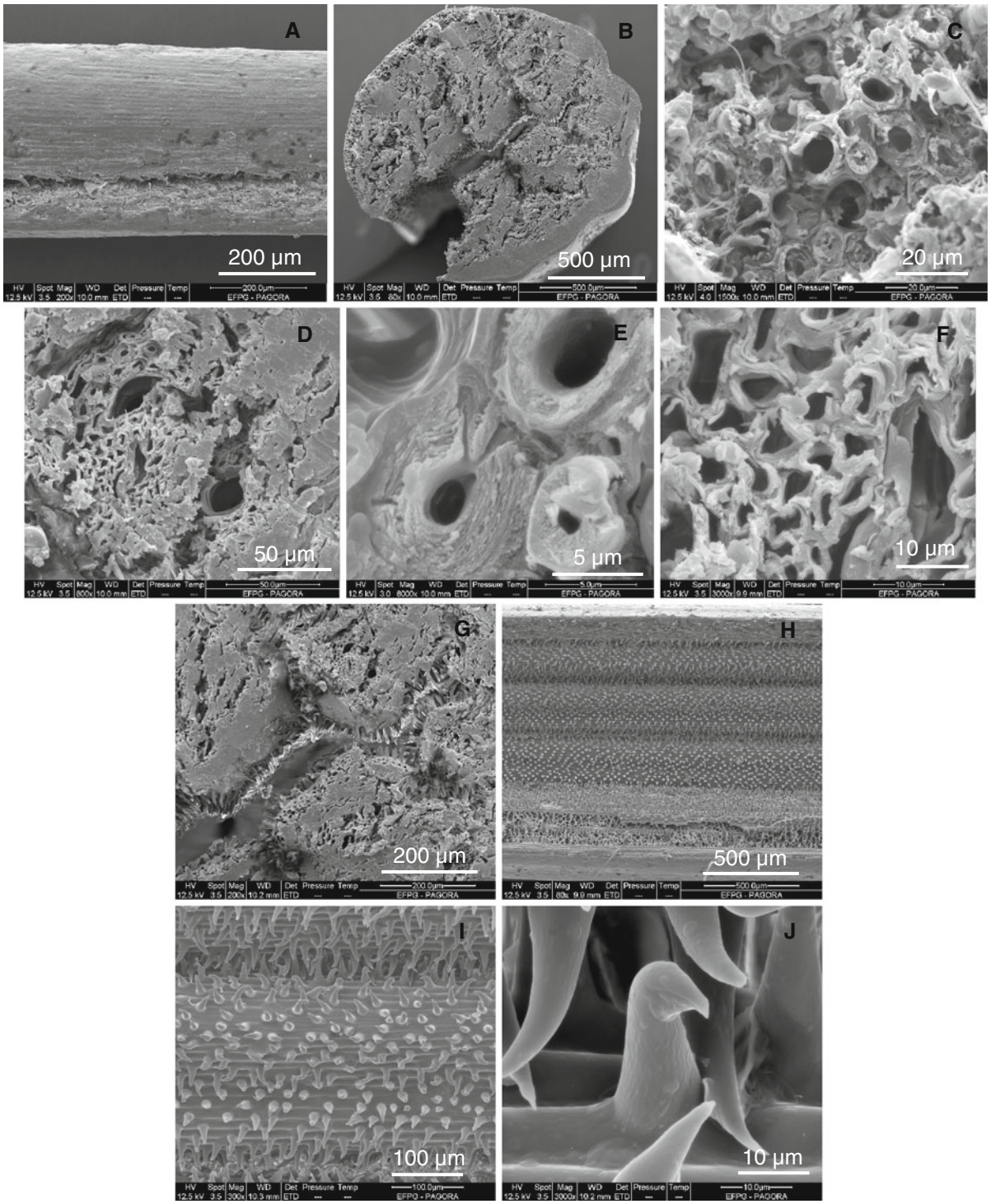

Fig. 1 Scanning electron micrographs showing the longitudinal view (**a**) and cross-section of alfa fibers (**b**), detailed structure of slot and the fiber bundles (**c**–**f**), slot structure (**g** and **h**), and detailed slot structure (**i** and **j**)

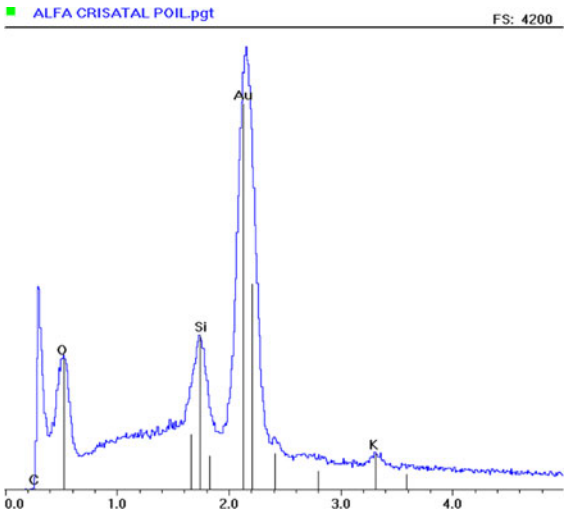

Fig. 2 Chemical analysis of the tips revealed in Fig. 1j determined by EDX-SEM

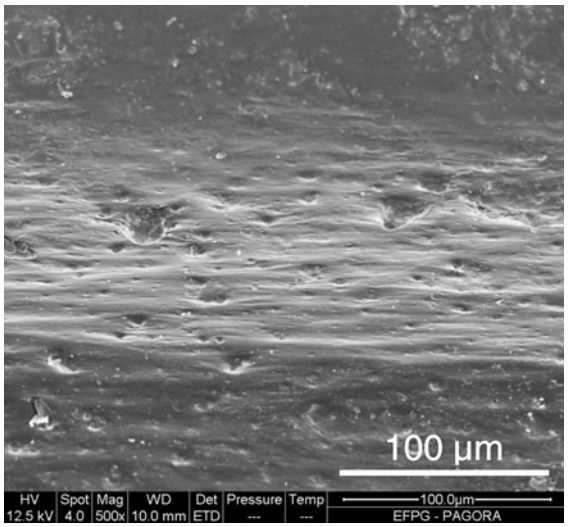

Fig. 3 Scanning electron micrograph of the surface of alfa fibers

being mainly formed of silica (Fig. 2). Although the fiber morphology was reported by Röser and Heklau (2011) and Bessadok et al. 2007 no indication about this inorganic structure was highlighted. Figures 3 show the SEM observation of the surface of the alfa fibers. The presence of stomata regularly dispersed on the surface is clearly visible.

Chemical composition and crystallinity

The constituents and chemical composition of alfa fibers are given in Table 1. The main constituents are polysaccharides (70 wt%), with about 45 wt% cellulose and 25% hemicelluloses. These results are consistent with those reported in the literature (Paiva et al. 2007; Ben Brahim and Ben Cheikh 2007; Bouiri and Amrani 2009). The polysaccharides content of alfa fibers is similar to the one obtained for the rachis of leaves of date palm tree (Bendahou et al. 2009, 2010; Khiari et al. 2010). However the lignin content is quite higher. It is also high compared to other annual plants such as jute or kenaf for which the lignin content is lower than 15 wt%.

To access the crystallinity of the fibers before and after the delignification treatment, wide angle X-ray diffraction measurements were carried out from which the crystallinity index was estimated according to Eq. 1. It was found to be around 57% for the pristine fibers, and about 85% after delignification and bleaching treatment. This was expected because of the amorphous structure of lignin and hemicelluloses.

Table 1 Chemical composition and crystallinity index (CrI) of alfa fibers

Constituent	Content (wt%)[a]
Ash	7.2 ± 1.0
Fat and wax	1.5 ± 0.3
Lignin	20 ± 2
Protein (N × 6.25)	1.1 ± 0.2
Cellulose	46 ± 3
Other polysaccharides	24 ± 2
CrI (raw alfa fibers)	57 ± 2%
CrI (delignified alfa fibers)	85 ± 3%

[a] As % of dry matter

Morphological investigation of CNC and MFC extracted from alfa fibers

Microfibrillated cellulose

The most common method adopted to induce the nanofibrillation of bleached delignified cellulose fibers and prepare MFC consists in submitting a suspension of cellulose fibers to high pressure homogenization until the break down of the hierarchical structure of cellulose fibers. However, applying this approach to alfa fibers was unfruitful even after 30 passes at 300 bars.

An activation treatment of the fibers called TEMPO-mediated oxidation was reported to be efficient for fibrillation giving rise to a strong gel after several passes at 300 bars. Actually, for carboxyl content around 300 ± 30 μmol/g, 10 passes were enough to get a consistent translucent gel (Besbes et al. 2011). Further passes at higher pressures (600 bars) did not result in any significant enhancement in the degree of transparency of the gel as shown in Fig. 4a. The relative low degree of transparency of the disintegrated alfa fibers is the result of the persistence of a relatively high amount of unfibrillated and partially fibrillated fraction responsible of light-scattering phenomenon. Based on centrifugation measurement the fraction of unfibrillated material was estimated to 68, 57 and 42% after 10 passes at 300 bars, 10 passes at 300 bars followed by 5 additional passes at 600 bars, and 10 passes at 300 bars followed by 15 additional passes at 600 bars, respectively.

To get a more accurate idea about the morphology of the ensuing fibrillated cellulose, FE-SEM investigations were carried out, by deposing a drop of the supernatant fraction of the MFC suspension (with a solid content between 0.05 and 0.1%) on a silicon wafer. It is worth noting that a centrifugation treatment of a diluted sample of the MCF gel at 4,500 rpm for 20 min (0.2% solid content) was necessary in order to separate the nanofibrillated material (in supernatant fraction) from non-fibrillated and partially fibrillated fibers which sedimented upon centrifugation. This treatment ensured better possibility to image the MFC using FE-SEM.

A FE-SEM image at high magnification of MFC obtained from alfa fibers is shown in Fig. 5a. The supernatant fraction of the ensuing MFC shows nanosized fibrils with a width being within the range of 5–20 nm. Further passes at higher pressure i.e. 600 bars did not modify the width of the fibrils, which could be an indication that the nanosized fibrils of the supernatant fraction correspond really to the inherent microfibrils.

The morphology of the sediment fraction of the MFC suspension is shown in Fig. 5b. Residual fibers fragments with widths ranging between 2 and 20 μm and lengths exceeding 50 μm are observed. At higher magnification an aggregated structure of microfibrils forming a highly entangled web-like layer is observed. These microfibrils were released and individualized after passing through the homogenizer, where the high shear forces break down the physical cohesion between the fibrils.

Cellulose nanocrystals

The dilute suspension of CNC extracted from alfa fibers gives a fully transparent dispersion showing a birefringent character when placed between cross-polarizers (Fig. 4b). It evidences the anisotropic orientation of CNC in the suspension giving rise to a liquid crystal-like behavior (Cranston and Gray 2008; Goetz et al. 2009). This phenomenon is also indicative of the good dispersion level of the cellulosic nano-rods ensured by the electrostatic repulsion among the fully ionized sulfate (SO_4^-) groups on the CNC surface.

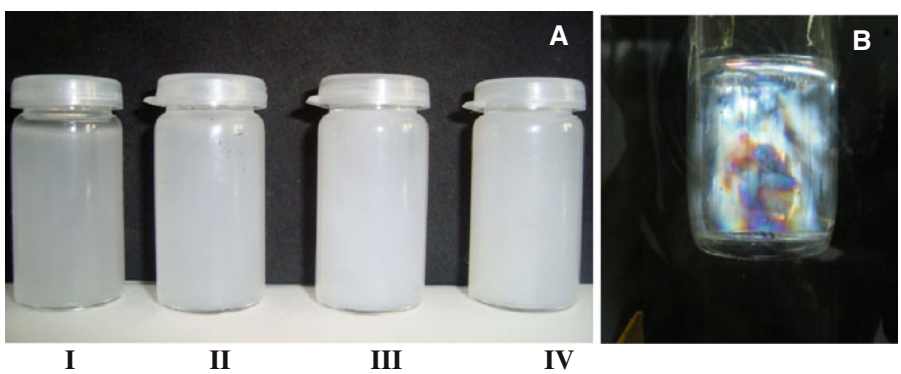

Fig. 4 Appearance of aqueous suspensions of MFC and CNC extracted from alfa fibers. (**a**) MFC gel (1 wt%) issuing from alfa fibers after (*I*) 10 passes at 300 bars, (*II*) 5 additional passes at 600 bars, (*III*) 10 additional passes at 600 bars and (*IV*) 15 additional passes at 600 bars. (**b**) CNC suspension (0.5 wt%) observed between cross-polarizers

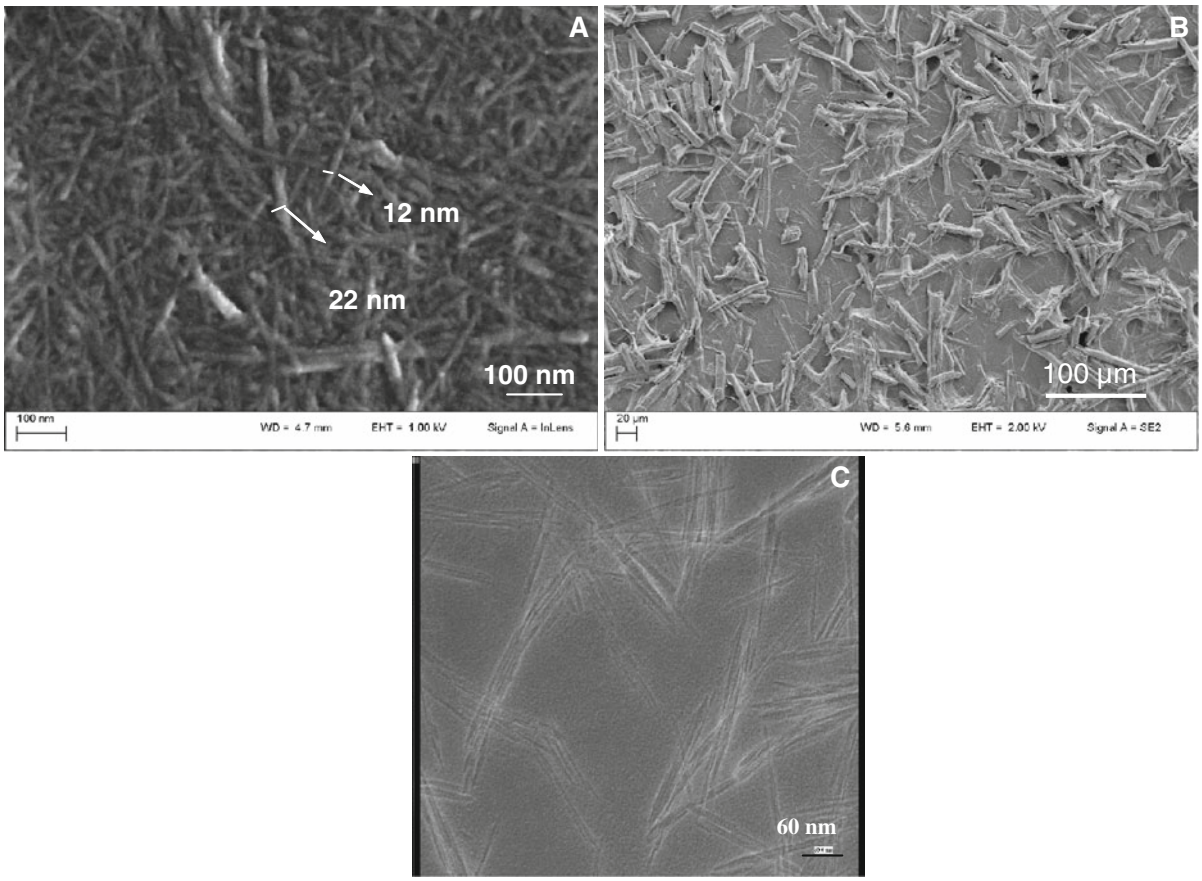

Fig. 5 FE-SEM pictures of (**a**) the supernatant fraction and (**b**) the sediment fraction of high-pressure homogenized alfa fibers after 5 passes at 300 bars, and (**c**) TEM picture of CNC extracted from alfa fibers

Figure 5c shows a TEM image of alfa CNC. It reveals a needle-like structure with a tendency to partial agglomeration by alignment of the whiskers along their main axis as the water is going off. The average length and width of alfa whiskers were estimated to be around 200 ± 20 and 10 ± 2 nm, respectively, giving an aspect ratio around 20. This latter value is low compared to the one of cellulose nanocrystals extracted from other plants like rachis of date palm tree (Bendahou et al. 2009, 2010), sisal (Siqueira et al. 2009), or *Luffa cylindrica* (Siqueira et al. 2010). However, it is higher compared to CNC extracted from cotton (de Souza Lima and Borsali 2004).

Mechanical properties of nanocomposite films

To investigate the reinforcement efficiency of the ensuing nanoparticles, nanocomposite films were prepared by casting mixture of an aqueous suspension of MFC (or CNC) and a commercial latex of poly(styrene-co-butyl acrylate). After water evaporation and polymer particles coalescence, the ensuing films were analyzed by DMA. The temperature dependence of the storage tensile modulus, E′, and tangent of the loss angle, tanδ, at 1 Hz for the unfilled poly(S-co-BA) matrix and nanocomposites with different CNC and MFC contents are shown in Fig. 6.

The curve of E′ corresponding to the unfilled poly(S-co-BA) matrix is typical of a fully amorphous polymer. For temperatures below the glass transition temperature, the polymer is in the glassy state and its storage modulus slightly decreases with temperature but remains roughly constant around 1 GPa. Then a sharp decrease of more than 3 decades is observed around 30 °C, corresponding to the main relaxation phenomenon which is associated to the anelastic

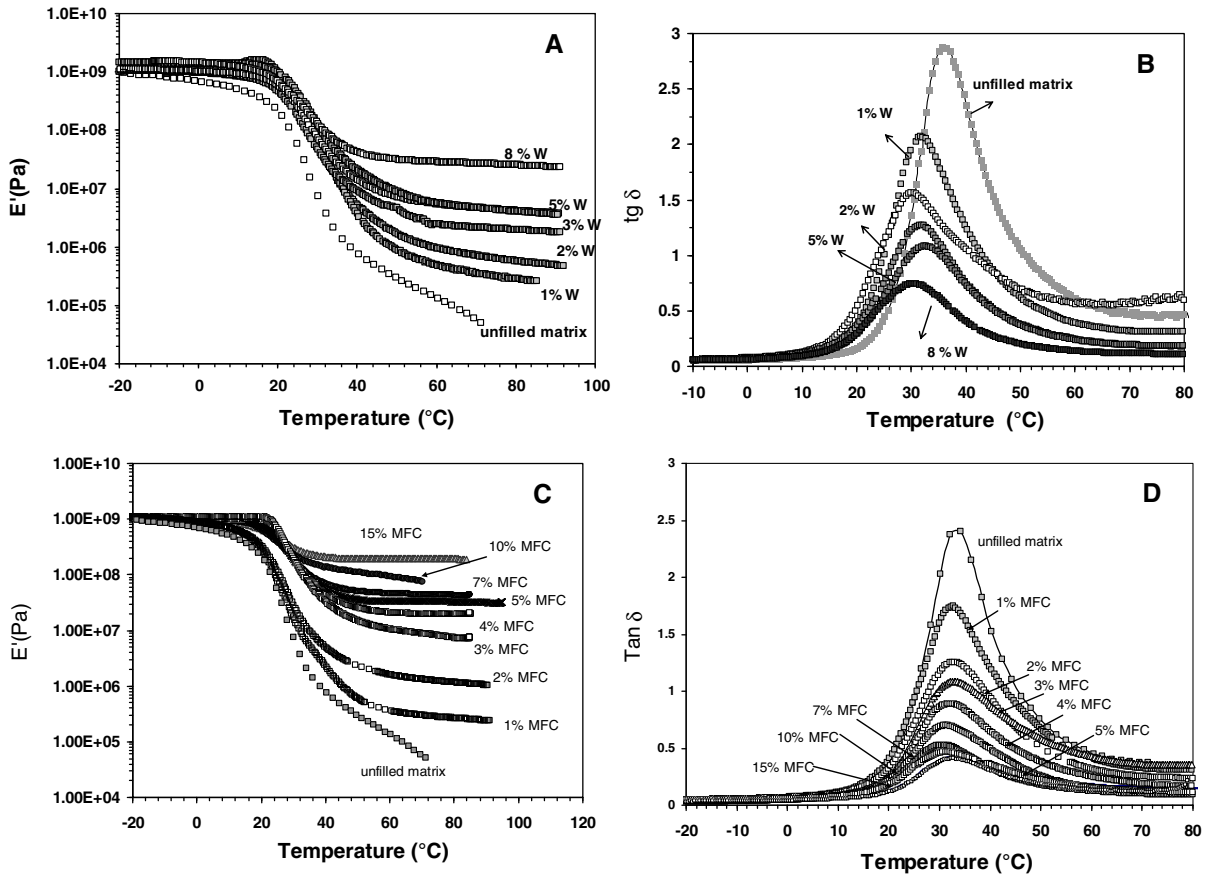

Fig. 6 Evolution of (**a**, **c**) the storage tensile modulus, E', and (**b**, **d**) tangent of the loss angle, tanδ, versus temperature at 1 Hz for nanocomposites based on CNC (**a**, **b**) and MFC (**b**, **d**) extracted from alfa fibers

manifestation of the glass transition. Then, the modulus reaches a plateau around 0.5 MPa. Around 35 °C, the loss angle shows a maximum (Fig. 6b, d) which magnitude is higher than the unity.

The temperature position of this relaxation process is slightly shifted towards lower temperatures. It is ascribed to the well known mechanical coupling effect. The magnitude of the relaxation process, which is related to the magnitude of the storage modulus drop, depends upon both the number of mobile entities and their contribution to the compliance. The relative damping is not related simply to the filler volume fraction but is also influenced by interfacial interactions. Strong interfacial interactions tend to create a layer of strongly adsorbed macromolecular chains in the interphase and to an apparent increase of the filler volume fraction. The strong decrease of the magnitude of the loss angle upon nanofibers addition is most probably related to adhesion between the filler and the matrix (Dufresne 2000).

For both sets of nanocomposites, the low temperature storage modulus did undergo only a slight enhancement with respect to the unfilled matrix (Fig. 6a, c). This is quite expected given the relatively low volume fraction of the reinforcing phase. On the contrary, above the glass transition the storage modulus increased significantly upon nanoparticle addition, which is in line with the well-known reinforcing effect of cellulosic nanoparticles.

To get a more insight on the stiffening effect of nanoparticles, the relative modulus defined as:

$$E_r = \frac{E_{\text{com}}}{E_{\text{mat}}}. \tag{2}$$

with E_{com} and E_{mat} being the storage moduli of the nanocomposite and unfilled matrix, respectively,

measured at 70 °C, i.e. around Tg + 40 °C, was determined. The evolution of E_r as a function of the nanoparticle content is shown in Fig. 7. The continuous rise in the relative modulus clearly confirmed the strong reinforcing effect of the prepared nanoparticles. However the trend of the reinforcing potential differs when comparing the two types of nanoparticles. Actually, it is more important in the case of MFC. As an example, the modulus is about 100 times and 20 times higher than that of the unfilled matrix after the addition of 4 wt% alfa MFC and CNC, respectively.

This higher reinforcing effect of MFC compared to CNC could be explained by the difference of structure of both nanoparticles. In fact, two parameters are responsible for the higher reinforcing effect of MFC. The first parameter is the higher aspect ratio of MFC which enables the formation of cellulose network at lower filler content. The second parameter is the possibility of entanglement of MFC owing to their flexibility. In the case of CNC only percolation of the nanocrystals is expected to bring reinforcement. The percolation threshold, ϕ_c, is inversely proportional to the aspect ratio (L/d) (Azizi Samir et al. 2005):

$$\phi_c = \frac{0.7}{L/d} \tag{3}$$

For alfa CNC with an aspect ration around 20, the percolation threshold is found to be close to 3.5 vol%, i.e. around 5.75 wt% taking 1 and 1.5 g.cm^{-3} for the density of the matrix and filler, respectively. For MFC, this value is difficult to estimate because of the ill-defined structure of the filler. Thus the lower reinforcing effect of alfa CNC reported in Fig. 7 could be attributed to their lower aspect ratio. The higher aspect ratio of MFC along with its flexible structure resulted in the formation of an entangled network for low filler content. However, it seems that above 6 wt% CNC the reinforcing capability of the rod-like nanoparticles seems to increase more sharply than for MFC.

The effect of the aspect ratio could be emphasized when comparing the reinforcing effect of CNC extracted from alfa ($L/d = 20$) and those extracted from the rachis of date palm tree ($L/d = 43$) (Bendahou et al. 2009). For the latter, the percolation threshold was estimated around 1.6 vol%, i.e. 2.4 wt%. It is clearly observed from Fig. 7 that the reinforcing effect of CNC extracted from the rachis of the date palm tree is higher compared to the one of CNC obtained from alfa fibers.

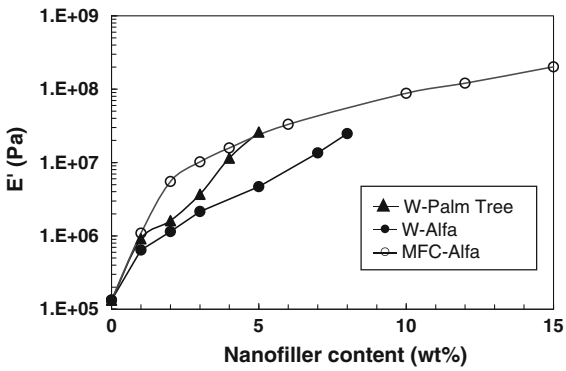

Fig. 7 Evolution of the relative storage modulus versus nanoparticle content at 70 °C for nanocomposite films prepared from CNC and MFC obtained from alfa fibers and acrylic latex. Data corresponding to CNC obtained from the rachis of date palm tree and natural rubber are added for comparison (Bendahou et al. 2009)

Conclusion

The microstructure and chemical composition of alfa (*Stipa tenacissima*) have been investigated. It was found that the alfa plant is composed of the sclerenchyma fibers (died cells or mature cells or tracheids) and conducting vessels. Moreover, alfa plant is wound on itself and the inner surface is covered with silica with pretty spectacular forms. The chemical composition analysis showed that the polysaccharide fraction is high and the fraction of lignin is about 20 wt%. The average length and width of cellulose nanocrystals extracted from alfa by acid hydrolysis treatment were estimated to be around 200 ± 20 and 10 ± 2 nm; the aspect ratio being therefore about 20. Microfibrillated cellulose was prepared using a combination of oxidative and mechanical treatments and showed a width within the range of 5–15 nm. These cellulosic nanoparticles have been used to prepare nanocomposite films using an acrylic polymer as matrix. Films were obtained by casting/evaporation. The thermo-mechanical properties of the ensuing nanocomposite films have been investigated using DMA. A significant increase of the stiffness of the acrylic polymer beyond the glass transition temperature was shown. MFC showed higher reinforcing effect compared to cellulose nanocrystals, probably because of higher aspect ratio and possibility of entanglement of the former.

Acknowledgments The authors thank for their financial support Hassan II Academy of Sciences and Techniques, the French Ministry of Foreign Affairs (Corus program 6046), the PHC-UTIQUE (Grant 11/G 1115) and the Tunisian Ministry of Higher Education and Scientific Research.

References

Azizi Samir MAS, Alloin F, Dufresne A (2005) Review of recent research into cellulosic whiskers, their properties and their application in nanocomposite field. Biomacromolecules 6:612–626

Ben Brahim S, Ben Cheikh R (2007) Influence of fiber orientation and volume fraction on the tensile properties of unidirectional Alfa polyester composite. Compos Sci Technol 67:140–147

Bendahou A, Habibi Y, Kaddami H, Dufresne A (2009) Physico-chemical characterization of palm from phoenix dactylifera–L, preparation of cellulose whiskers and natural rubber–based nanocomposites. J Biobased Mat Bioenerg 3:1–10

Bendahou A, Kaddami H, Dufresne A (2010) Investigation on the effect of cellulosic nanoparticles morphology on the properties of natural rubber based nanocomposites. Eur Polym J 46:609–620

Besbes I, Alila S, Boufi S (2011) Nanofibrillated cellulose from TEMPO-oxidized eucalyptus fibres: effect of the carboxyl content. Carbohydr Polym 84:975–983

Bessadok A, Marais S, Gouanve F, Colasse L, Zimmerlin I, Roudesli S, Métayer M (2007) Effect of chemical treatments of alfa (Stipa tenacissima) fibres on water-sorption properties. Compos Sci Technol 67:685–697

Bouiri B, Amrani M (2009) Production of dissolving grade pulp from alfa. BioResources 5:291–302

Cranston ED, Gray DG (2008) Birefringence in spin-coated films containing cellulose nanocrystals. Col Surf A 325:44–51

de Souza Lima M, Borsali R (2004) Rodlike cellulose microcrystals: structure, properties, and applications. Macromol Rapid Comm 25:771–774

Dufresne A (2000) Dynamic mechanical analysis of the interphase in bacterial polyester/cellulose whiskers natural composites. Compos Interfaces 7:53–67

Dufresne A (2008) Polysaccharide nanocrystals reinforced nanocomposites. Can J Chem 86:484–494

Frisch HL, Mark EJ (1996) Nanocomposites prepared by threading polymer chains through zeolites, mesoporous silica, or silica nanotubes. Chem Mater 8:1735–1738

Goetz L, Mathew A, Oksman K, Gatenholm P, Ragauskas AJ (2009) A novel nanocomposite film prepared from cross-linked cellulosic whiskers. Carbohydr Polym 75:85–89

Harris PJF (2004) Carbon nanotube composites. Int Mater Rev 49:31–43

Kaddami H, Gérard JF, Pascault JP (2004) Influence of the initiation rate on the polymerization kinetics of hydroxy ethyl methacrylate (HEMA) filled with HEMA-grafted silica preformed nanoparticles. Polym Eng Sci 44:1231–1939

Kaddami H, Becker-Villinger C, Schmidt H (2006) Monitoring morphology and properties of hybrid organic-inorganic materials from in situ polymerization of tetraethoxysilane in polyimide polymer: 1) effect of the coupling agent on the microstructure and interfacial interaction. E-Polymers 10:1–10

Khiari R, Mhenni MF, Belgacem MN, Mauret E (2010) Chemical composition and pulping of date palm rachis and *Posidonia oceanica* – A comparison with other wood and non-wood fibre sources. Biores Technol 101:775–780

Lau KT, Gu C, Hui D (2006) A critical review on nanotube and nanotube/nanoclay related polymer composite materials. Composites B 37:425–436

Motomatsu M, Takahashi T, Nie HY, Mizutani W, Tokumoto H (1997) Microstructure study of acrylic polymer-silica nanocomposite surface by scanning force microscopy. Polymer 38:177–182

Okada A, Kawasumi M, Usuki A, Kojima Y, Kurauchi T, Kamigaito O (1990) Nylon 6-clay hybrid. Mater Res Soc Proc 171:45–50

Paiva MC, Ammar I, Campos AR, Ben Cheikh R, Cunha AM (2007) Alfa fibers: mechanical, morphological and interfacial characterization. Compos Sci Technol 67:1132–1138

Pit Z, Mark EJ, Jethmalani JM, Ford WT (1996) Mechanical properties of a poly(methvl acrvlate) nanocomposite containing regularly-arranged silica particles. Polym Bull 37:545–551

Röser M, Heklau H (2011) Abscission of leaf laminas—an unnoticed factor in tussock grass formation. Flora 206: 32–37

Ruckenstein E, Yuan Y (1997) Nanocomposites of rigid polyamide dispersed in flexible vinyl. Polymer 38:3855–3860

Saito T, Hirota M, Tamura N, Kimura S, Fukuzumi H, Heux L, Isogai A (2009) Individualization of nano-sized plant cellulose fibrils by direct surface carboxylation using TEMPO catalyst under neutral conditions. Biomacromolecules 10:1992–1996

Segal L, Creely JJ, Martin AE, Conrad CM (1959) An empirical method for estimation the degree of crystallinity of native cellulose using the X-ray diffractometer. Textile Res J 29: 786–794

Siqueira G, Bras J, Dufresne A (2009) Cellulose whiskers versus microfibrils: influence of nature of the nanoparticle and its surface functionalization on the thermal and mechanical properties of nanocomposites. Biomacromolecules 10: 425–432

Siqueira G, Bras J, Dufresne A (2010) *Luffa cylindrica* as a lignocellulosic source of fiber, microfibrillated cellulose, and cellulose nanocrystals. BioResources 5727–740

Sirò I, Plackett D (2010) Microfibrillated cellulose and new nanocomposites materials: a review. Cellulose 17:459–494

Terre et Vie (2002), L'Alfa : Importance écologique et socio-économique, N° 61–62. (http://www.terrevie.ovh.org/Alfa.pdf)